Potential permafrost distribution and ground temperatures based on surface state obtained from microwave satellite data

Christine Kroisleitner[1,2], Annett Bartsch[1,2,3], and Helena Bergstedt[4,2]

[1]Zentralanstalt für Meteorologie und Geodynamik, Vienna, Austria
[2]Austrian Polar Research Institute, Vienna, Austria
[3]b.geos, Korneuburg, Austria
[4]Salzburg University, Austria

Correspondence to: Annett Bartsch (annett.bartsch@zamg.ac.at)

Abstract. A threshold of half a year frozen conditions has been previously suggested for the determination of potential permafrost extent from a passive microwave sensor using 37 GHz (SSM/I). We argue that this value should be higher and needs to be refined. Further on, data using lower frequencies such as from Metop ASCAT (5.3 GHz) might be more suitable. We used borehole temperature records from across the Arctic for the assessment. The comparison to mean annual ground temperature

5 (MAGT) at coldest sensor depth revealed that temperature can be directly obtained from ASCAT surface state with a residual error of 2.5°C compared to 3°C in case of SSM/I. The optimum threshold of frozen days to estimate permafrost extent is 190 days for SSM/I, as determined in comparison to borehole data (Kendall's τ test), and 196 days from modelled MAGT. Thresholds for Metop ASCAT are 204 and 212 frozen days per year respectively. Data sets are comparably coarse (12.5km - 25km nominal resolution) and the accuracy of the modelled MAGT varies regionally but the approach does not require gap

10 filling or spatial interpolation as in the case of conventional frozen ground modelling from temperature measurements.

1 Introduction

Permafrost covers large parts of the Earth's surface and is defined as ground that remains at or below 0°C for at least two
consecutive years. The impact of climate change on the Arctic, as well as other permafrost dominated environments, is thought
to be more severe compared to the rest of the world (Schuur et al., 2015; National research Council, 2013). Warming and

5 with that thawing of permafrost impacts multiple environmental processes ranging from surface and sub-surface hydrology
(O'Donnell et al., 2012; Woo et al., 2008), ecological changes (Schuur et al., 2008) to processes like carbon exchange (Hayes
et al., 2014). Knowledge of the extent of permafrost and possible changes in it's distribution are therefor crucial for climate
modelling and prediction (Cheng and Wu, 2007; O'Connor et al., 2010). So far, the exact extend of permafrost is unknown and
has only been approximated (Zhang et al., 2008; Nguyen et al., 2009).

10 A range of approaches exist for permafrost extent determination. They vary in complexity, accuracy and their parameteriza-
tion differs depending on the size of the area of interest and data availability. Different temperature data sources are employed
for the approximation. E.g. Gruber (2012) uses re-analyses records, which are based on spatially interpolated in situ air tem-
perature data (mean annual air temperature) together with elevation data (laps rate), to generate a global map of permafrost
probabilities. Temperature records from re-analyses and land surface temperature from satellites together with basic vegeta-

15 tion information and satellite derived snow properties have been investigated for modelling larger areas by Westermann et al.
(2015). Satellite data alone do not provide the required spatially and temporally consistent temperature values. Cloud cover is
problematic when using thermal infrared. Clear sky bias is an additional problem (Soliman et al., 2012). Improved temperature
records can be obtained for the snow free period from combination with passive microwave data (André et al., 2015) but they
need to be complemented with re-analysis data for the remaining year in order to derive the required indices.

20 A different and simpler approach using only satellite records has been recently described by Park et al. (2016). They hy-
pothesize that the number of frozen days per year from passive microwave satellite data (SSM/I - Special Sensor Microwave
Imager) can be used as indicator for permafrost extent. A 30 year record was analyzed for trends and compared to the map of
Brown et al. (1997) - often referred to as the IPA (International Permafrost Association) map - and results of the CHANGE
progress model (Park et al., 2011a). A threshold of half a year of frozen days during at least two consecutive years was chosen

25 to delineate possible permafrost areas. This value was justified with reference to Dobinski (2011), Nelson and Outcalt (1987),
Saito et al. (2013) and Zhang et al. (2005). These studies use measures derived from actual temperature records, specifically
the use of mean annual air temperature and the concept of thawing/freezing degree days. Results showed differences between
the model and microwave product, especially at the start of the record which could be due to sparse satellite data during the
beginning of the chosen time period (Trofaier et al., 2017). The comparison with the IPA permafrost map revealed an overesti-

30 mation of permafrost extent around 65°N. Overall, agreement regionally differed, especially over non-continuous permafrost.
Luoto et al. (2004) suggest that the minimum number of frozen days is 200 for new permafrost to develop (in form of palsas)
in the transition zone of Scandinavia. Additionally, local factors like a low annual mean temperature (<1°C), water-saturated
peat, moss patches and low vegetation have to be present (Seppälä, 1986; Harris, 1981). This number is considerably higher,
compared to the selection of Park et al. (2016).

Surface state information can be also derived from active microwave sensors operating at various frequencies (Park et al., 2011b; Naeimi et al., 2012; Bartsch et al., 2007; Wang et al., 2008; Zwieback et al., 2015) and with that the calculation of frozen and thawed days per year. Frequencies are usually lower than SSM/I and especially C-band (5.3 GHz) scatterometer like the ASCAT (Advanced Scatterometer) sensor on-board the Metop satellites have already been shown to be applicable for
5 freeze-thaw information retrieval in permafrost regions by validation with near surface soil temperature from borehole records (Naeimi et al., 2012). Multi-annual statistics of thaw and freeze-up timing based on these records have been e.g. applied for the retrieval of circumpolar landscape units (Bartsch et al., 2016).

The objective of this study is the determination of the validity of the half year threshold for the approach presented by Park et al. (2016) and assessment of the performance of active microwave data with a lower frequency. We implement the
10 approach suggested for passive microwave records (SSM/I) for data obtained by the ASCAT sensor. The sensitivity analyses is supported by the permafrost distribution map by Brown et al. (1997) and in situ borehole temperature measurements. The number of frozen days is further directly compared to borehole records within different permafrost types to establish an empirical relationship, which can then be used to 1) alternatively separate between frozen and unfrozen based on the zero degree temperature threshold and 2) provide a spatially continuous estimate of potential ground temperatures.

2 Datasets

2.1 Satellite records

We used two microwave remote sensing data sets derived from globally available records and with similar classification accuracy obtained by comparison to air temperature data. They are derived from sensors with different frequencies, acquisition methods (active versus passive) and timing. The first was derived from the ASCAT sensor on-board the Metop satellites. The
20 ASCAT sensor is a C-band (5.255 GHz) scatterometer (Figa-Saldaña, et al., 2002), providing almost daily coverage of the Earth's surface. The equator overpass time is 9:30 am. The surface state information (freeze/thaw) has been derived from the ASCAT sensor as a surface status flag for a soil moisture product specifically post-processed for high latitudes (Paulik et al., 2014). The circumpolar data set covers the years 2007 - 2013. It was developed for permafrost monitoring and climate modelling purposes (Bartsch and Seifert, 2012; Naeimi et al., 2012; Reschke et al., 2012), and covers the area above 50°N with
25 a grid spacing of 12.5 km and an up to daily temporal resolution (Paulik et al., 2014). This includes the parameters frozen and thawed ground, temporary water (including snow melt) and frozen water/permanent ice. The surface status information was derived using a step-wise threshold algorithm based on ASCAT backscatter values and ECMWF ReAnalyis data (Naeimi et al., 2012). The accuracy was assessed with in situ surface air temperature measurements from the global weather station network and found to be about 82% overall (Naeimi et al., 2012). Up to 92% agreement was found for near surface temperature
30 measurements from boreholes of the Global Terrestrial Network on Permafrost (GTN-P) located in Siberia.

The second remotely sensed data set used in this study was derived from global daily (ascending and descending orbit) 37 GHz, vertically polarized brightness temperature observations from calibrated SMMR (scanning multi-channel microwave radiometer) and SSM/I (special sensor microwave imager) satellite sensor records by Kim et al. (2014). There have been a

series of those sensors carried on-board satellites from the Defense Meteorological Satellite Program. They are passive radiometric systems that measure atmospheric, ocean and terrain microwave temperature (Hollinger et al., 1990). SSM/I equatorial crossings are 6 am and 6 pm. The freeze-thaw status was analyzed globally from 1979 - 2012 by Kim et al. (2014). The data set has a nominal resolution of 25 km and covers the Arctic terrestrial drainage basin. The actual footprint size at 37GHz is

5 37km x 28km. The threshold approach produces two classes: frozen and non-frozen. The estimated classification accuracy is approximately 85% (am passes) to 92% (pm passes) compared to in situ surface air temperature measurements from the global weather station network (Kim et al., 2012). It has been used by Park et al. (2016) for the assessment of permafrost extent changes.

2.1.1 In situ records

10 All borehole records above a latitude of 50° North with available time series of ground temperature were retrieved from the Global Terrestrial Network for Permafrost database (GTN-P, 2016). The network collects measurements of the Thermal State of Permafrost (TSP) in polar and mountain regions. 277 borehole sites have temperature data, single sites often comprise more then one measurement unit or period, which leads to a total sum of 1062 ground temperature data sets (Biskaborn et al., 2015). The depth of most boreholes is less than 25 m, although the average lies at 53 m. The most frequent sensor depth is found

15 at 5 m. Permanently installed multi-thermistor cables showing an accuracy between 0.002 - 0.1°C are most commonly used for measuring continuous ground temperatures at specific depths (Romanovsky et al., 2010). The time series are available in hourly, daily or annual resolution and cover different time periods. Deepest sensor depths of the used data set vary between 1m and 140m. In total 265 boreholes have been considered. They represent a Mean Annual Ground Temperature (MAGT) range from -17.7°C to 10°C. There are however inconsistencies in sensor spacing and the MAGT at zero annual temperature

20 amplitude is not directly measured. Most records of North America are accompanied with meta records which suggest es sensor depth for approximation of the MAGT. But this information is unavailable for the majority of records from Asia.

2.1.2 Map of permafrost extent

The circumpolar permafrost map by Brown et al. (1997) depicts the permafrost extent divided in different classes as well as the ground ice content for the Northern Hemisphere (20°N to 90°N). The data set defines permafrost as frozen ground that remains

25 at or below 0°C for at least two years. Areas are classified as continuous, discontinuous, sporadic or isolated permafrost with differing ground ice content. The classes correspond to percent area categories: 90-100%, 50-90%, 10-50%, <10%, and no permafrost. These classes have been compared separately and as one aggregated class (excluding areas of no permafrost) to the results of the frozen day classifications.

3   Methods

3.1   Preparation of borehole temperature data

The mean annual ground temperature (MAGT) is usually calculated at the depth of zero annual amplitude (ZAA) for permafrost studies. As the availability of data at specific depths is limited, representing or reaching the depth of ZAA is not possible for

5   all cases. The MAGT, defined as the temperature at a specific site in this study, was therefore calculated for each borehole location at the depth of the minimum MAGT. The minimum MAGT, in a stable climate, would be the same as the MAGT at the depth of ZAA, but due to climate variations the coldest annual temperature is often recorded below the ZAA (Lachembruch and Marshall, 1986). We found the MAGT at the depth of the coldest value better reproducible while still comparable to the MAGT at ZAA. Temperature time series of the different sensors have been tested for gaps and inconsistencies. We included

10   shallow boreholes (<1m), mainly situated in areas showing no permafrost, in order to carve out the relationship between the MAGT and the amount of days of year frozen at the location. About half of the records represent locations with -5 to 0°C at coldest sensor depth.

3.2   Pre-processing of satellite records

Both surface status data sets underwent post-processing before being used in our permafrost extent and temperature estimation.

15   The ASCAT surface status flag (SSF) data contain cells with no data where the algorithm failed to produce a result. Gaps were filled by surrounding values (class with majority), ensuring a complete data set. The sum of frozen days per year for every pixel was determined for both satellite records, according to the method of Park et al. (2016). Grid cells where the number of frozen days exceeds the number of thawed days during two consecutive years are classified as permafrost. We have defined the averaging period with respect to the water year from September 1 to August 31 as suggested by Park et al. (2016).

20   To explore the dependency of the results on snow melting events, the permafrost extent estimation from ASCAT data was carried out excluding the melt days in the count of frozen days (FT) and a second analysis counting the melt days as frozen grid cells (FM).

3.3   Frozen days threshold determination for permafrost extent

In the study of Park et al. (2016) a threshold of half a year was chosen for the delineation of permafrost extent. Half year

25   corresponds to 180 or 182.5 days in climate models (Saito et al., 2013). In a first step, we extended the analysis to 210 frozen days to test the validity of the suggested threshold. The cross comparison with the permafrost extent classes considers the information of four thresholds (180, 190, 200, 210) for the entire study area what allowed us to analyze the difference in estimated permafrost extent and the sensitivity of this approach to the chosen threshold. The results from both active and passive microwave freeze/thaw data sets were compared with the permafrost map by Brown et al. (1997).

30   To evaluate the initial threshold of half a year with in situ data, ASCAT and SSM/I data were extracted for each of the borehole locations. We classified borehole (coldest sensor) derived MAGT > 0 as 0 and MAGT <= 0 as 1 and the DOY >

"threshold" as 1 and DOY < "threshold" as 0. Kendall's Tau (τ) was used to examine the correlation coefficient between the in situ and satellite derived data set. It was chosen as it provides a method to measure the ordinal association to measured or calculated quantities. In order to determine the most suitable limit to map permafrost extent, thresholds where varied from 180 to 210 days in one day steps. For the evaluation of the initial threshold of 180 days we divided the dataset (all years and

5   stations) into four sectors; positive and negative MAGT versus DOY >= 180 and DOY < 180. The number of considered data points differ between SSM/I and ASCAT due to different masking schemes.

3.4   Model parametrization for ground temperature retrieval

The relationship between MAGT and frozen day of year was further examined for the retrieval of ground temperature and consecutive determination of permafrost extent by using the 0°C threshold. Only data inside the range of 150 to 330 frozen

10   DOY have been considered. Additionally, sites which are located on islands in the high Arctic have been excluded with respect to microwave sensor footprint size. The remaining 168 sites haven been used to fit the model. The records from ASCAT as well as SSM/I have been split into two parts by defining a calibration (2010-2012) and a validation period (2008-2009). We tested linear, logarithmic and polynomial functions on their ability to describe the relationship between MAGT and day of year frozen. We found no significant fit for polynomial functions and a slightly weaker fit for logarithmic functions compared to

15   a simple linear regression. Therefore a linear model has been applied to the frozen days for the years 2010 to 2012 for the determination of an empirical relationship. The resulting formula was used to estimate the MAGT from the day of year data set for the years 2008 and 2009. The differences between the modelled and in situ MAGT have been calculated separately for the two years in order to assess the capability of the approach to capture inter-annual variations. The Arctic has been split up into 12 regions for this purpose (Fig. A1).

20   ## 4   Results

4.1   Threshold sensitivity analyses and permafrost extent

The area mapped as permafrost with a frozen day threshold of 180 days for the period 2007-2012 differs regionally between the ASCAT and the SSM/I data set (Fig. 1). The classification using SSM/I data results in a smaller permafrost extent for the Canadian Arctic compared to Brown et al. (1997). The ASCAT map shows comparably good agreement in this region. On the

25   other hand, ASCAT overestimates the permafrost extent in Scandinavia. There is more year to year variability in the results from the analysis using SSM/I data. The largest deviation in area extent for continuous permafrost occurs in the SSM/I result with more than 2.5 Mio km2 (more than 12 %, Fig. 2). Less than 1 Mio km^2 (less than 5% of total continuous permafrost area) is missed by ASCAT in case of thresholds between 180 and 200 frozen days which exclude snow melt days. Matching extent is lower for 200 days in case of inclusion of snow melt days. ASCAT maps more permafrost outside the boundaries of

30   Brown et al. (2007) than SSM/I in case of a 180 day threshold but agrees better than SSM/I for discontinuous and isolated

Table 1. Comparison matrix between in situ Mean Annual Ground Temperature (MAGT, at coldest sensor depth) classes (below or above zero °C) and classified number of frozen days per year from ASCAT (FT - excluding snow melt days, FM - including snow melt days) and SSM/I for 2007-2012. Both, the initial 180 Days of Year (DOY) threshold and the optimal threshold based on best Kendall's τ are assessed. Values represent numbers of sites for multiple years. Rows indicating false classifications are in *italic*.

Sensor	ASCAT FT		ASCAT FM		SSM/I	
DOY	**180**	**204**	**180**	**203**	**180**	**190**
Positive MAGT & DOY <thres.	142	210	127	194	112	142
Negative MAGT & DOY <thresh.	*2*	*79*	*0*	*34*	*24*	*54*
Positive MAGT & DOY >= thresh.	*122*	*54*	*137*	*70*	*144*	*114*
Negative MAGT & DOY >= thresh.	574	497	576	542	452	422
Sum of data points	840	840	840	840	732	732

Table 2. Comparison between in situ Mean Annual Ground Temperature (MAGT, at coldest sensor depth) with number of frozen days per year from ASCAT (FT - excluding snow melt days, FM - including snow melt days) and SSM/I for 2007-2012.

Parameter	ASCAT FT	ASCAT FM	SSM/I
Pearson correlation for linear fit	0.62	0.60	0.30
Residual standard error for linear fit	2.483	2.535	3.109
DOY for zero degree C from linear fit	212	206	196
DOY for best Kendall's τ	204	203	190

permafrost area. This results in lower percentage agreement of the SSM/I product for the total permafrost extent (Fig. 3). The false permafrost detection by ASCAT is out-weighted by a significantly higher detection performance for the total extent.

For the ASCAT data sets the best τ was found to coincide with 204 (FT) and 203 (FM) frozen DOY (Fig. 1), whereas for the SSM/I 190 DOY showed the highest τ with a steep gradient before and after the peak (Fig. 4).

5   More locations with positive MAGT fall in areas with values above the threshold for both ASCAT results than for SSM/I (Fig. 1). It is highest for exclusion of snow melting days. On the other hand the ASCAT results show nearly no negative MAGT below the threshold of 180. The thresholds delineated by the best correlation coefficient (Kendall's τ) indicate for all data sets a better performance regarding positive MAGT in areas below the threshold. However, the higher thresholds lead also to more negative MAGT in these areas. For the SSM/I 77% of MAGT temperatures can be correctly allocated with both thresholds.

10 The ASCAT results show a higher accuracy with more than 80% correctly assigned values.

4.2   Mean annual ground temperature

The Pearson correlation for the linear fit decreases slightly from 0.62 to 0.60 if snow melting days are excluded (Fig. 5 and Table 2). The same applies to the residual standard error (2.48 versus 2.53). The slope of the linear fit also differs slightly between the two ASCAT data sets (Fig. 5). It is steeper in case of exclusion of melting days as well as for SSM/I. The spread

of in situ temperature values is higher for conditions below 0°C than above. This is similar for all data sets. The majority of MAGT values (in a wide range of -10°C to 5°C) are found in the sector between 170 and 250 frozen DOY for ASCAT. The Pearson correlation in case of SSM/I is lower with 0.3 and residual standard error is higher with 3°C (Fig. 6). A difference of 11 frozen days of near surface soil corresponds to 1°C in case of ASCAT FT.

5   There are no significant differences in model performance between 2008 and 2009 (Fig. 7 and 8). The FT and FM methods differ more for the year 2007 than for 2008 (Fig. 8 and 9). The SSM/I extent misses a large proportion of continuous permafrost and maps additional area as permafrost (more pronounced in 2007, Fig. 9), similarly to the initial threshold based comparison to the permafrost extent map (Fig. 2).

The largest spatial differences between included/excluded melting days occur in the same regions (Northeastern Canada
10   and Scandinavia), which show the largest differences between the ASCAT and SSM/I 180 day threshold maps (Fig. 10). An additional region of disagreement is central Yakutia. The inclusion of snow melting days leads here to a reduction of permafrost extent which is contradictory to most other regions.

The modelled extent and best Kendall's τ threshold results correspond largely to continuous permafrost (Fig. 10). The exclusion of melting snow has a large impact over Scandinavia. It leads to results which are more similar to the map of Brown
15   et al. (1997). It is also one of the regions with extensive snow melt detected by ASCAT (Fig. A2). Patterns of continuous permafrost in central Asia (e.g. region around lake Baikal) are better represented in the ASCAT maps than in the SSM/I retrievals. The same applies to northwestern Russia, west of the Ural mountains.

The deviations of ASCAT results from in situ records differ for most regions between the two validation years (Fig. 11). They are only similar for Greenland and Svalbard. These sites show the highest deviations. The differences of the ASCAT
20   FT results are mostly in the order of one degree Celsius for other regions, except the Yamal-Nenets district and northern Sweden. The deviations of the SSM/I product are largest in central Russia, Yakutsk region and the Yamal-Nenets district. This is consistent with the patterns observed in comparison to the permafrost map (Fig. 10). Three of the borehole sites in the validation/calibration dataset which are defined as continuous permafrost in the meta records and are located away from coastlines have positive temperatures in both validation years in the ASCAT result: Umaybyt, Shapkina (Bolvansky), and
25   Tunka (Buryat). All are located close to the boundary of continuous permafrost. About 20 sites of the full GTN-P records had positive temperatures although being classified as continuous.

The inclusion of days with melting snow reduces the deviations in Sweden, Yamal-Nenets district, East Siberia, Alaska and the Canadian Arctic, but increases for central Siberia, Yakutsk and especially in the transition zone of Western Russia. The difference between the ASCAT products is here more than three degree Celsius. The model result is about two degree colder
30   than what is obtained from the in situ records.

The average difference is below one degree Celsius for all three products. The modelled result tends to be warmer than the in situ records for most regions, what is also reflected in the overall average.

5   Discussion

The performance of the empirical model for MAGT (coldest sensor) is partially lower than what can be achieved with the more complex TTOP model (Westermann et al., 2015) which considers terrain, snow, land cover and land surface temperature measurements from satellite data. Westermann et al. (2015) reported a model accuracy of 2.5°C. There are several stations
5   which have a DOY that corresponds to modelled temperatures between 0°C to -5°C, but in situ MAGT between -5°C and -10°C. They are located on high latitude islands, the Brooks Range in Alaska and Central Yakutia. The deviations are most likely due to the coarse spatial resolution which cannot resolve the spatial heterogeneity in these areas resulting from high water fraction and topographic range. Location specific soil properties may also play a role, specifically for peatlands in the transition zones. The lower performance of SSM/I might be attributed to the fact that it has an even larger footprint (although
10   gridded to 25km) than ASCAT. The instruments also differ in wavelength apart from the fact that one is active and the other passive. ASCAT uses C-band with about 5.7 cm and the SSM/I channel used by Park et al. (2016) about 0.8 cm. This results in different signal interactions with objects on the earth surface including snow and vegetation. It can be expected that the C-band signal is less sensitive to interactions, although present.

    A threshold higher than the previously suggested half year leads to better performance of ASCAT especially over Scan-
15   dinavia, west of the Ural mountains and Eastern Russia (Chabarovsk region). Results suggest that days with melting snow should be treated as unfrozen. It is expected that temperatures within a snow pack are around 0°C as long as melting lasts. The ground below is however impacted. Mid winter melt has been shown previously to alter ground temperatures (Westermann et al., 2011). Spring snow melt detected by satellites also coincides with initiation of soil processes. Rising CO_2 fluxes can be measured (Bartsch et al., 2007, 2010). The number of snow melting days are in general highly variable in the Arctic (Bartsch,
20   2010). They are not mapped for all grid points in case of the ASCAT data set (Fig. A2). This may depend on snow depth as well as acquisition timing. The coverage pattern is irregular across the Arctic with a mix of morning and evening (ascending and descending orbits) measurements (Bergstedt and Bartsch, 2017). Usually only evening measurements capture the melt as diurnal freeze and thaw cycles are common (Bartsch et al., 2007). The differentiation between frozen and melting days may however be valid in regions with prolonged melt. Areas with melting snow in the ASCAT data set are common in the high
25   Arctic, in areas with low MAGT (Fig. A2) as well as areas in the transitions zone (such as Scandinavia). This pattern differs from the length of the snow melt period detected with Seawinds QuikScat, a Ku-band scatterometer (Bartsch, 2010), which provides several measurements per day. The number of days with snow melt are much lower in C-band than in the Ku-band product. This could be attributed to the lower sensitivity of C-band to melting processes and the limited temporal sampling. In addition, the QuikScat results in Bartsch (2010) are representing periods of freezing and thawing which can contain breaks
30   (with frozen conditions) of up to ten days.

    The overall extent of permafrost estimated with the initial threshold is in the order of the actual extent but the error of commission is relatively large. ASCAT better captures the regional patterns except for Scandinavia. The actual temperature amplitude (freezing and thawing degree days) may need to be considered in this region. The longer snow melt period (Fig. A2) also indicates a certain amount of snow which may lead to decoupling of air and ground temperatures. Permafrost temperatures

are also not always representing current climate conditions (Lachembruch and Marshall, 1986). This may regionally impact the comparability of the borehole records with surface observations. Estimates of permafrost temperatures as well as extent are therefore providing a potential distribution only. Results may however support the identification of regions where permafrost extent maps, including continuity classes, need to be refined. Year to year variations need to be, however, treated with care.

5   The highest density of boreholes with available data is in the Vorkuta region in Western Siberia/Russia. This region shows the largest sensitivity to inclusion/exclusion of snow melting days. The ASCAT results differ here by more than two degree Celsius (lower temperature). This might have an impact on the average deviation derived from the entire borehole records. It is likely larger for the ASCAT FM result than calculated as most other regions have higher modelled temperature values.

The Greenland and Svalbard sites are expected to have the highest variations due to the mixture of glaciers, land area and
10   ocean within the ASCAT as well as SSM/I pixels. There is actually no coverage of the Greenland sites in the SSM/I records. The validation results are therefore not fully comparable between the sensors for the entire Arctic, only on regional level. This may also affect the calibration, since the number of available samples is lower for SSM/I. In general, less areas are masked in the ASCAT product. This applies to especially lake rich regions. Findings of Bergstedt and Bartsch (2017) suggest an offset of the state change in the resolution cell due to lakes. This may lead to lower accuracy in these regions.

15   The majority of boreholes located in the regions 'Central Russia' and 'Central Siberia' show higher than zero degree MAGT. The validation results differ from those of the other areas. ASCAT as well as SSM/I results suggest between one to two degree lower MAGT values. Most of these boreholes are shallower than five meter what might influence the MAGT as derived in this study. The mean annual ground temperature from boreholes was calculated from the coldest sensor below 1 m. The depth of these sensors varies from borehole to borehole what may impact the empirical model representativity. A high number of sites
20   has been however chosen for calibration what may weaken the impact. This is supported by a DOY threshold of the best fit close to the one defined by the Kendall's τ test.

The in all cases (ASCAT and SSM/I, for all methods) higher accounts of number of frozen days than the previously suggested half year threshold agrees with field observations by Luoto et al. (2004), who estimated a minimum number of 200 days for permafrost formation for Scandinavia. 200 days corresponds to approximately 0.5°C in case of ASCAT FT. Considering local
25   factors such as water-saturated peat and organic layer and uncertainties in the retrieval (difference to actual mean temperature), this might still be counted as sufficient for permafrost formation. Variations of topography within the footprint lead also to local deviations from days to weeks (Bergstedt and Bartsch, 2017). We therefore suggest the consideration of temperature buffers (see example of ±1° range in Fig. 7) when such data are applied. Boreholes with in situ MAGT below 0°C located in these buffer zones may represent sites where local factors are important. The role of past climate conditions for present ground
30   temperatures need to be considered in addition.

The reduction of permafrost extent in case of exclusion of melting days (FT) for the ground temperature retrieval from ASCAT is the result of the slight difference in slope of the linear function compared to FM. The range of borehole temperatures for locations with approximately 200 frozen days is also much larger than for smaller or higher DOY numbers (Fig. 5). Results suggest that SSM/I freeze/thaw records are less suitable to derive actual MAGT values below zero degree Celsius (Fig. 6). The
35   thresholds obtained for SSM/I are considerably lower than for ASCAT, what might be the result of the different wavelength, the

sensing technique (passive/active), overpass timing and classification methods used to create these data sets. The considerable lower number of frozen days in regions with low MAGT might be the result of the retrieval method (treatment regarding acquisition timing) and sensitivity to soil state changes. The latter issue could be addressed by L-band missions with even lower frequency than ASCAT such as SMOS (Soil Moisture and Ocean Salinity Mission) or SMAP (Soil Moisture Active and

5 Passive). In general, the role of acquisition timing and sampling rate needs to be investigated in more detail for permafrost related applications for ASCAT as well as SSM/I.

The classes in Brown et al. (1997) correspond to area fraction of permanently frozen ground. In case of the isolated permafrost class it can be assumed that at least 10% are below 0°C, but the actual mean temperature for a region in these areas (as e.g. represented by an ASCAT or SSM/I cell) can be below or above 0°C depending on local parameters such as topography

10 and soil properties which impact thermal conductivity. The latter plays especially a role for occurrence of permafrost in the transition zone. Higher spatial resolution data sets would be required. Relevant measurements from microwave data are only available from active systems due to technical constraints. Synthetic Aperture Radar (SAR) instruments could be used in case of sufficient sampling intervals (Park et al., 2011b). Current systems and acquisition plans do however not provide a sufficient sampling, temporally and spatially (Bartsch et al., 2016).

15 **6   Conclusions**

All four approaches point to a higher number of frozen days threshold than 180 days for the determination of permafrost extent: (1) the quantification of area overlap with the permafrost map by Brown et al. (1997), (2) Kendall's τ test using borehole measurements (Fig. 4), (3) in situ data matrix using borehole measurements (Table 1) as well as (4) the direct comparison to in situ MAGT at coldest sensor depth (Table 2). This applies not only to the ASCAT data but also to the SSM/I data for which a

20 half year threshold has been initially proposed.

The direct comparison to borehole temperatures reveals the potential of C-band scatterometer based surface status detection for ground temperature estimation. A linear empirical model can be applied when days with melting snow are excluded. The modelled temperature deviates on average by less than one degree Celsius in footprints without glaciers and mix of land and ocean. Especially regions with large variations of frozen days between the years and/or between the three different

25 products (ASCAT with snow melting days and without, the SSM/I records) need to be further investigated with respect to the representativity of the borehole records and derived temperatures respectively. They mostly correspond to the permafrost transition zones. The validity of the coarse resolution microwave satellite records for the point locations needs to be confirmed by e.g. using higher spatial resolution synthetic aperture radar (SAR) records. More detailed analyses of the role of melting snow conditions is required in addition. Conventional approaches for spatially continuous mapping of permafrost temperatures

30 require gap filling or spatial interpolation. The C-band radar record provides a purely observational account.

7 Data availability

The average annual sums of frozen and snow melting days derived from Metop ASCAT are available via the ESA DUE GlobPermafrost project WebGIS and catalogue. www.globpermafrost.info.

Author contributions. CK has performed all data analyses and contributed to the preparation of figures. The concept of the paper was jointly
5 developed by CK and AB. AB wrote the majority of manuscript. CK contributed to the writing of the in situ, methods and results sections, HB to the satellite data description and discussion.

Competing interests. The authors declare no conflict of interest

Acknowledgements. This work was supported by the Austrian Science Fund (Fonds zur Förderung der wissenschaftlichen Forschung, FWF) under Grant [I 1401] (Joint Russian–Austrian project COLD-Yamal), Grant [DK W1237-N23] (Doctoral College GIScience) as well as the
10 European Space Agency project DUE GlobPermafrost (contract number 4000116196/15/I-NB).

References

André, C., Ottlé, C., Royer, A., and Maignan, F.: Land surface temperature retrieval over circumpolar Arctic using SSM/I–SSMIS and MODIS data, Remote Sensing of Environment, 162, 1 – 10, doi:10.1016/j.rse.2015.01.028, 2015.

Bartsch, A.: Ten Years of SeaWinds on QuikSCAT for Snow Applications, Remote Sensing, 2, 1142–1156, doi:10.3390/rs2041142, 2010.

5 Bartsch, A. and Seifert, F. M.: The ESA DUE Permafrost project - A service for high latitude research, in: 2012 IEEE International Geoscience and Remote Sensing Symposium, pp. 5222–5225, doi:10.1109/IGARSS.2012.6352432, 2012.

Bartsch, A., Kidd, R. A., Wagner, W., and Bartalis, Z.: Temporal and Spatial Variability of the Beginning and End of Daily Spring Freeze/Thaw Cycles Derived from Scatterometer Data, Remote Sensing of Environment, 106, 360–374, doi:10.1016/j.rse.2006.09.004, 2007.

10 Bartsch, A., Wagner, W., and Kidd, R.: Remote Sensing of Spring Snowmelt in Siberia, in: Environmental Change in Siberia. Earth Observation, Field Studies and Modelling, edited by Balzter, H., pp. 135–155, Springer, doi:10.1007/978-90-481-8641-9_9, 2010.

Bartsch, A., Höfler, A., Kroisleitner, C., and Trofaier, A. M.: Land Cover Mapping in Northern High Latitude Permafrost Regions with Satellite Data: Achievements and Remaining Challenges, Remote Sensing, 8, 979, doi:10.3390/rs8120979, 2016.

Bartsch, A., Kroisleitner, C., and Heim, B.: Circumpolar Landscape Units, links to GeoTIFFs, doi:10.1594/PANGAEA.864508, https://doi.
15 pangaea.de/10.1594/PANGAEA.864508, supplement to: Bartsch, A et al. (2016): An Assessment of Permafrost Long-term monitoring sites with circumpolar satellite derived datasets. Proceedings of the ESA Living Planet Symposium 2016. ESA SP-740, Prague, Czech Republic, 6 pp, hdl:10013/epic.48548.d001, 2016.

Bergstedt, H. and Bartsch, A.: Surface State across Scales; Temporal and SpatialPatterns in Land Surface Freeze/Thaw Dynamics, Geosciences, 7, 65, doi:10.3390/geosciences7030065, 2017.

20 Biskaborn, B. K., Lanckman, J.-P., Lantuit, H., Elger, K., Streletskiy, D. A., Cable, W. L., and Romanovsky, V. E.: The new database of the Global Terrestrial Network for Permafrost (GTN-P), Earth System Science Data, 7, 245–259, doi:10.5194/essd-7-245-2015, 2015.

Brown, J., Ferrians, Jr., O., Heginbottom, J., and Melnikov, E.: Circum-Arctic map of permafrost and ground-ice conditions, 1997.

Brown, R., Derksen, C., and Wang, L.: Assessment of Spring Snow Cover Duration Variability over Northern Canada From Satellite Dataset, Remote Sensing of Environment, 111, 367–381, 2007.

25 Cheng, G. and Wu, T.: Responses of permafrost to climate change and their environmental significance, Qinghai-Tibet Plateau, Journal of Geophysical Research: Earth Surface, 112, doi:10.1029/2006JF000631, 2007.

Dobinski, W.: Permafrost, Earth-Science Reviews, 108, 158 – 169, doi:10.1016/j.earscirev.2011.06.007, 2011.

Figa-Saldaña,, J., Wilson, J., Attema, E., Gelsthorpe, R., Drinkwater, M., and Stoffelen, A.: The advanced scatterometer (ASCAT) on the meteorological operational (MetOp) platform: A follow on for European wind scatterometers, Canadian Journal of Remote Sensing, 28,
30 404–412, doi:10.5589/m02-035, 2002.

Gruber, S.: Derivation and analysis of a high-resolution estimate of global permafrost zonation, The Cryosphere, 6, 221–233, doi:10.5194/tc-6-221-2012, 2012.

GTN-P: Global Terrestrial Network for Permafrost Database: Permafrost Temperature Data (TSP Thermal State of Permafrost), 2016.

Harris, S. A.: Distribution of zonal permafrost landforms with freezing and thawing indices, Erdkunde, 35, 81–90,
35 doi:10.3112/erdkunde.1981.02.01, 1981.

Hayes, D. J., Kicklighter, D. W., McGuire, A. D., Chen, M., Zhuang, Q., Yuan, F., Melillo, J. M., and Wullschleger, S. D.: The impacts of recent permafrost thaw on land–atmosphere greenhouse gas exchange, Environmental Research Letters, 9, 045 005, 2014.

Hollinger, J. P., Peirce, J. L., and Poe, G. A.: SSM/I instrument evaluation, IEEE Transactions on Geoscience and Remote Sensing, 28, 781–790, doi:10.1109/36.58964, 1990.

Kim, Y., Kimball, J. S., Zhang, K., and McDonald, K. C.: Satellite detection of increasing Northern Hemisphere non-frozen seasons from 1979 to 2008: Implications for regional vegetation growth, Remote Sensing of Environment, 121, 472–487, 2012.

5   Kim, Y., Kimball, J. S., Glassy, J., and McDonald, K. C.: MEaSUREs Global Record of Daily Landscape Freeze/Thaw Status, Version 3, doi:10.5067/MEASURES/CRYOSPHERE/nsidc-0477.003, 2014.

Lachembruch, A. H. and Marshall, B. V.: Changing climate: geothermal evidence from permafrost in the Alaskan Arctic, Science, 234, 689 – 696, 1986.

Luoto, M., Fronzek, S., and Zuidhoff, F. S.: Spatial modelling of palsa mires in relation to climate in northern Europe, Earth Surface Processes

10   and Landforms, 29, 1373–1387, doi:10.1002/esp.1099, 2004.

Naeimi, V., Paulik, C., Bartsch, A., Wagner, W., Kidd, R., Boike, J., and Elger, K.: ASCAT Surface State Flag (SSF): Extracting Information on Surface Freeze/Thaw Conditions from Backscatter Data Using an Empirical Threshold-Analysis Algorithm, IEEE Transactions on Geoscience and Remote Sensing, 50, 2566–2582, doi:10.1109/TGRS.2011.2177667, 2012.

National research Council: Abrupt impacts of climate change: Anticipating surprises, National Academies Press, 2013.

15   Nelson, F. E. and Outcalt, S. I.: A Computational Method for Prediction and Regionalization of Permafrost, Arctic and Alpine Research, 19, 279–288, 1987.

Nguyen, T., Burn, C., King, D., and Smith, S.: Estimating the extent of near surface permafrost using remote sensing, Mackenzie Delta, Northwest Territories, Permafrost and Periglacial Processes, 20, 141–153, doi:10.1002/ppp.637, 2009.

O'Connor, F. M., Boucher, O., Gedney, N., Jones, C. D., Folberth, G. A., Coppell, R., Friedlingstein, P., Collins, W. J., Chappellaz, J., Ridley,

20   J., and Johnson, C. E.: Possible role of wetlands, permafrost, and methane hydrates in the methane cycle under future climate change: A review, Reviews of Geophysics, 48, n/a–n/a, doi:10.1029/2010RG000326, rG4005, 2010.

O'Donnell, J. A., Jorgenson, M. T., Harden, J. W., McGuire, A. D., Kanevskiy, M. Z., and Wickland, K. P.: The Effects of Permafrost Thaw on Soil Hydrologic, Thermal, and Carbon Dynamics in an Alaskan Peatland, Ecosystems, 15, 213–229, doi:10.1007/s10021-011-9504-0, 2012.

25   Park, H., Iijima, Y., Yabuki, H., Ohta, T., Walsh, J., Kodama, Y., and Ohata, T.: The application of a coupled hydrological and biogeochemical model (CHANGE) for modeling of energy, water, and CO2 exchanges over a larch forest in eastern Siberia, Journal of Geophysical Research: Atmospheres, 116, doi:10.1029/2010JD015386, d15102, 2011a.

Park, H., Kim, Y., and Kimball, J.: Widespread permafrost vulnerability and soil active layer increases over the high northern latitudes inferred from satellite remote sensing and process model assessments, Remote Sensing of Environment, pp. 349–358,

30   doi:10.1016/j.rse.2015.12.046, 2016.

Park, S.-E., Bartsch, A., Sabel, D., Wagner, W., Naeimi, V., and Yamaguchi, Y.: Monitoring Freeze/Thaw Cycles Using ENVISAT ASAR Global Mode, Remote Sensing of Environment, 115, 3457–3467, 2011b.

Paulik, C., Melzer, T., Hahn, S., Bartsch, A., Heim, B., Elger, K., and Wagner, W.: Circumpolar surface soil moisture and freeze/thaw surface status remote sensing products (version 4) with links to geotiff images and NetCDF files (2007-01 to 2013-12),

35   doi:10.1594/PANGAEA.832153, https://doi.pangaea.de/10.1594/PANGAEA.832153, 2014.

Reschke, J., Bartsch, A., Schlaffer, S., and Schepaschenko, D.: Capability of C-Band SAR for Operational Wetland Monitoring at High Latitudes, Remote Sensing, 4, 2923–2943, 2012.

Romanovsky, V., Smith, S., and Christiansen, H.: Permafrost Thermal State in the Polar Northern Hemisphere during the International Polar Year 2007-2009: a Synthesis, Permafrost and Periglac. Process., 21, 106–116, doi:10.1002/ppp.689, 2010.

Saito, K., Sueyoshi, T., Marchenko, S., Romanovsky, V., Otto-Bliesner, B., Walsh, J., Bigelow, N., Hendricks, A., and Yoshikawa, K.: LGM permafrost distribution: how well can the latest PMIP multi-model ensembles perform reconstruction?, Climate of the Past, 9, 1697–1714, doi:10.5194/cp-9-1697-2013, 2013.

Schuur, E., Bockheim, J., Canadell, J., and Euskirchen, E.: Vulnerability of permafrost carbon to climate change: Implications for the global carbon cycle, BioScience, doi:10.1641/B580807, 2008.

Schuur, E. A. G., McGuire, A. D., Schädel, C., Grosse, G., Harden, J. W., Hayes, D. J., Hugelius, G., Koven, C. D., Kuhry, P., Lawrence, D. M., Natali, S. M., Olefeldt, D., Romanovsky, V. E., Schaefer, K., Turetsky, M. R., Treat, C. C., and Vonk, J. E.: Climate change and the permafrost carbon feedback, Nature, 520, 171–179, doi:10.1038/nature14338, 2015.

Seppälä, M.: The origin of palsas, Geografiska Annaler. Series A. Physical Geography, 1986.

Soliman, A., Duguay, C., Saunders, W., and Hachem, S.: Pan-Arctic Land Surface Temperature from MODIS and AATSR: Product Development and Intercomparison, Remote Sensing, 4, 3833–3856, doi:10.3390/rs4123833, 2012.

Trofaier, A. M., Westermann, S., and Bartsch, A.: Progress in space-borne studies of permafrost for climate science: Towards a multi-ECV approach, Remote Sensing of Environment, doi:https://doi.org/10.1016/j.rse.2017.05.021, 2017.

Wang, L., Derksen, C., and Brown, R.: Detection of Pan-Arctic Terrerstrial Snowmelt from QuikSCAT, 2000-2005, Remote Sensing of Environment, 112, 3794–3805, 2008.

Westermann, S., Boike, J., Langer, M., Schuler, T. V., and Etzelmüller, B.: Modeling the impact of wintertime rain events on the thermal regime of permafrost, The Cryosphere, 5, 945–959, doi:10.5194/tc-5-945-2011, 2011.

Westermann, S., Østby, T., Gisnås, K., Schuler, T., and Etzelmüller, B.: A ground temperature map of the North Atlantic permafrost region based on remote sensing and reanalysis data, Cryosphere, 9, 1303–1319, doi:10.5194/tc-9-1303-2015, 2015.

Woo, M., Kane, D. L., Carey, S. K., and Yang, D.: Progress in permafrost hydrology in the new millennium, Permafrost and Periglacial Processes, 19, 237–254, doi:10.1002/ppp.613, 2008.

Zhang, T., Frauenfeld, O. W., Serreze, M. C., Etringer, A., Oelke, C., McCreight, J., Barry, R. G., Gilichinsky, D., Yang, D., Ye, H., Ling, F., and Chudinova, S.: Spatial and temporal variability in active layer thickness over the Russian Arctic drainage basin, Journal of Geophysical Research: Atmospheres, 110, n/a–n/a, doi:10.1029/2004JD005642, d16101, 2005.

Zhang, T., Barry, R., Knowles, K., Heginbottom, J., and Brown, J.: Statistics and characteristics of permafrost and ground-ice distribution in the Northern Hemisphere, Polar Geography, 31, 47–68, doi:10.1080/10889370802175895, 2008.

Zwieback, S., Paulik, C., and Wagner, W.: Frozen Soil Detection Based on Advanced Scatterometer Observations and Air Temperature Data as Part of Soil Moisture Retrieval, Remote Sens, 7, 3206–3231, doi:10.3390/rs70303206, 2015.
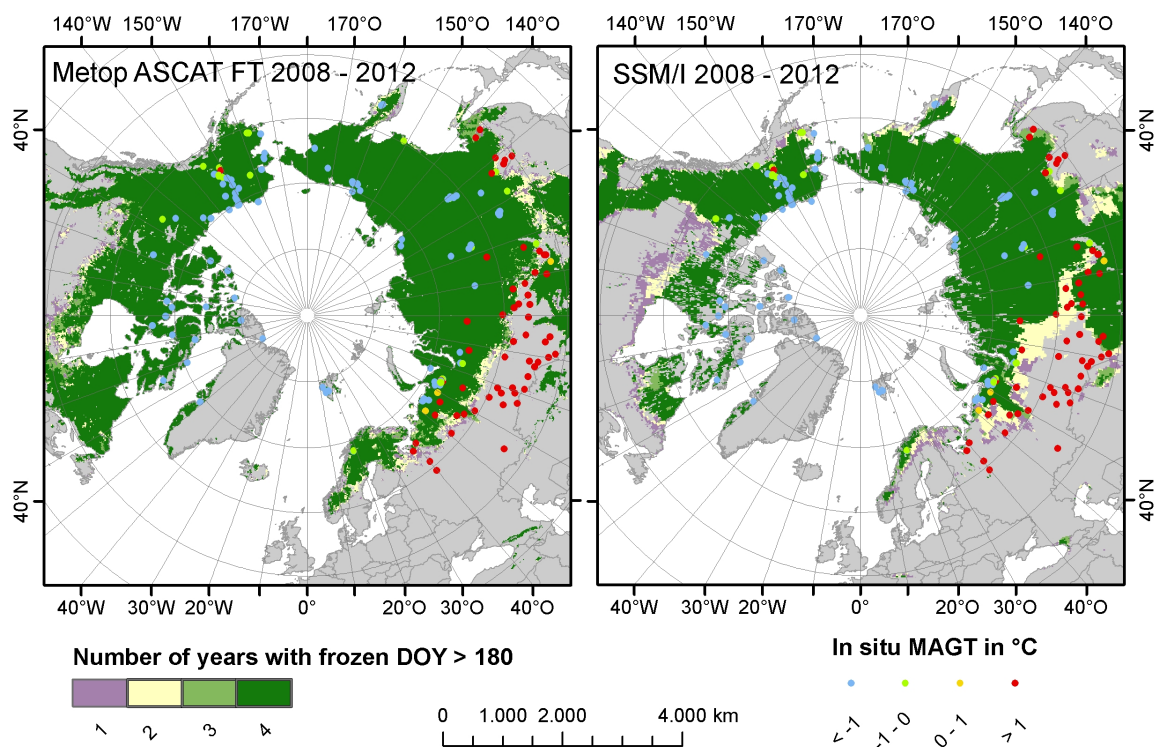
Figure 1. Permafrost extent comparison of satellite data results from Metop ASCAT and SSM/I for 2008-2012 based on the 180 day threshold method applied to all years (minimum of two consecutive years with at least 180 days frozen).
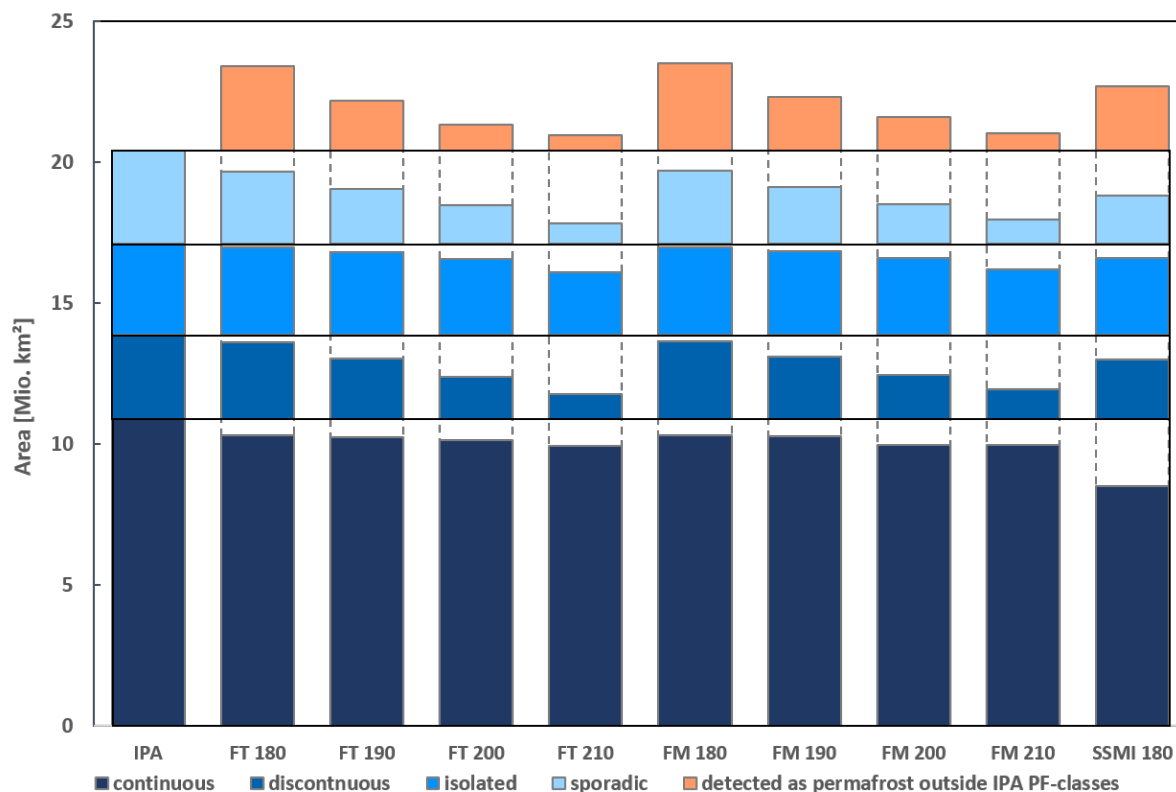
Figure 2. Permafrost extent comparison of satellite data results from Metop ASCAT based on modified thresholds (180, 190, 200 and 210 days) with permafrost extent classes from Brown et al. (1997). Covered area is provided in km^2 within each class. FT - days identified as frozen without melting snow are used, FM - days with melting snow are considered as frozen ground with Metop ASCAT. SSM/I classification results based on 180 days is included for comparison.
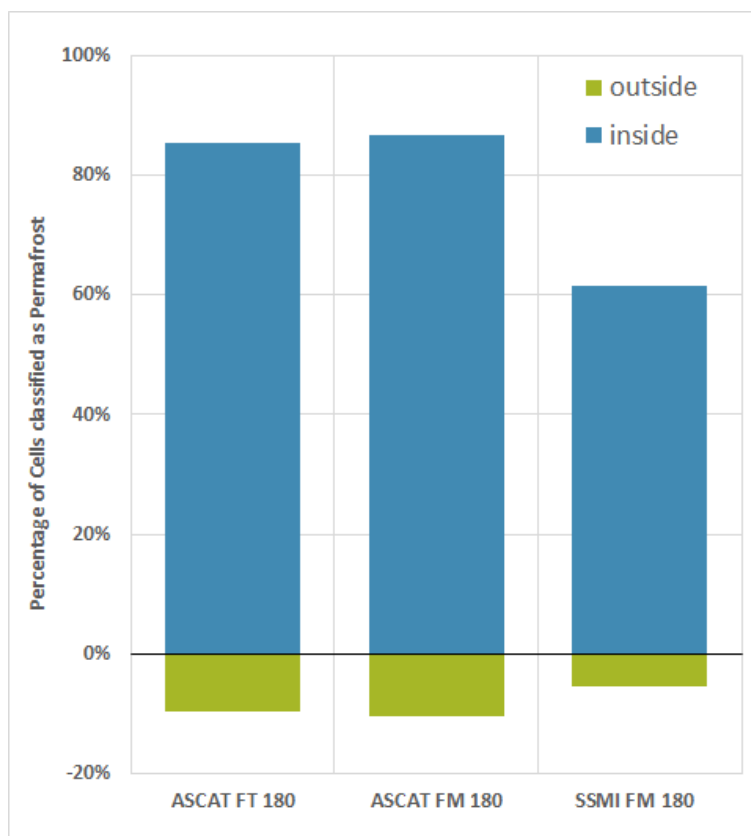
Figure 3. Comparison of satellite data results based on a 180 day threshold with permafrost extent from Brown et al. (2007). Covered area in % inside and outside permafrost regions is provided. FT - days identified as frozen without melting snow are used, FM - days with melting snow are considered as frozen ground with Metop ASCAT.
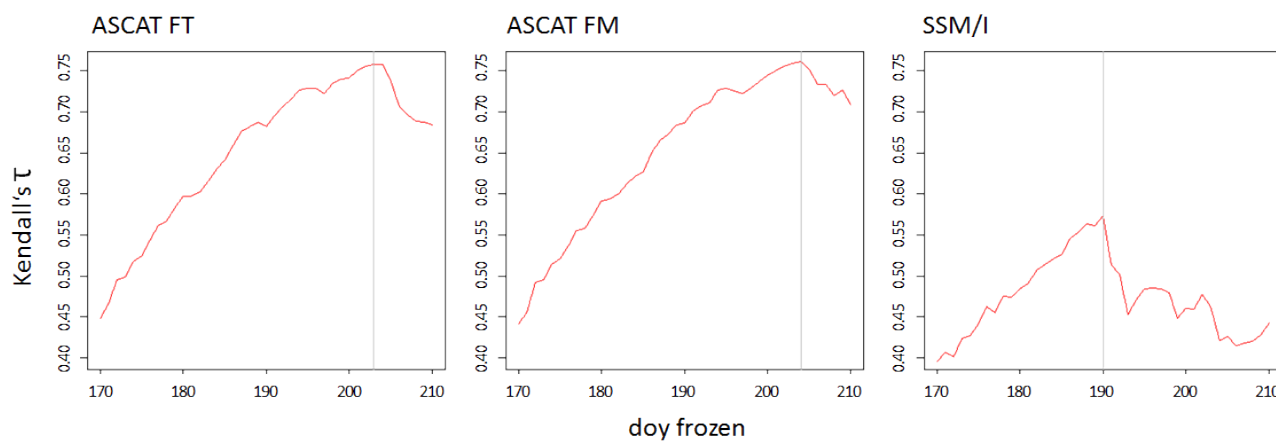
Figure 4. Curves of correlation coefficient (Kendall's τ) between 180 and 210 day of year (doy) frozen from satellite products and positive or negative MAGT at depth of coldest sensor from borehole data. FT - days identified as frozen without melting snow are used, FM - days with melting snow are considered as frozen ground with Metop ASCAT.
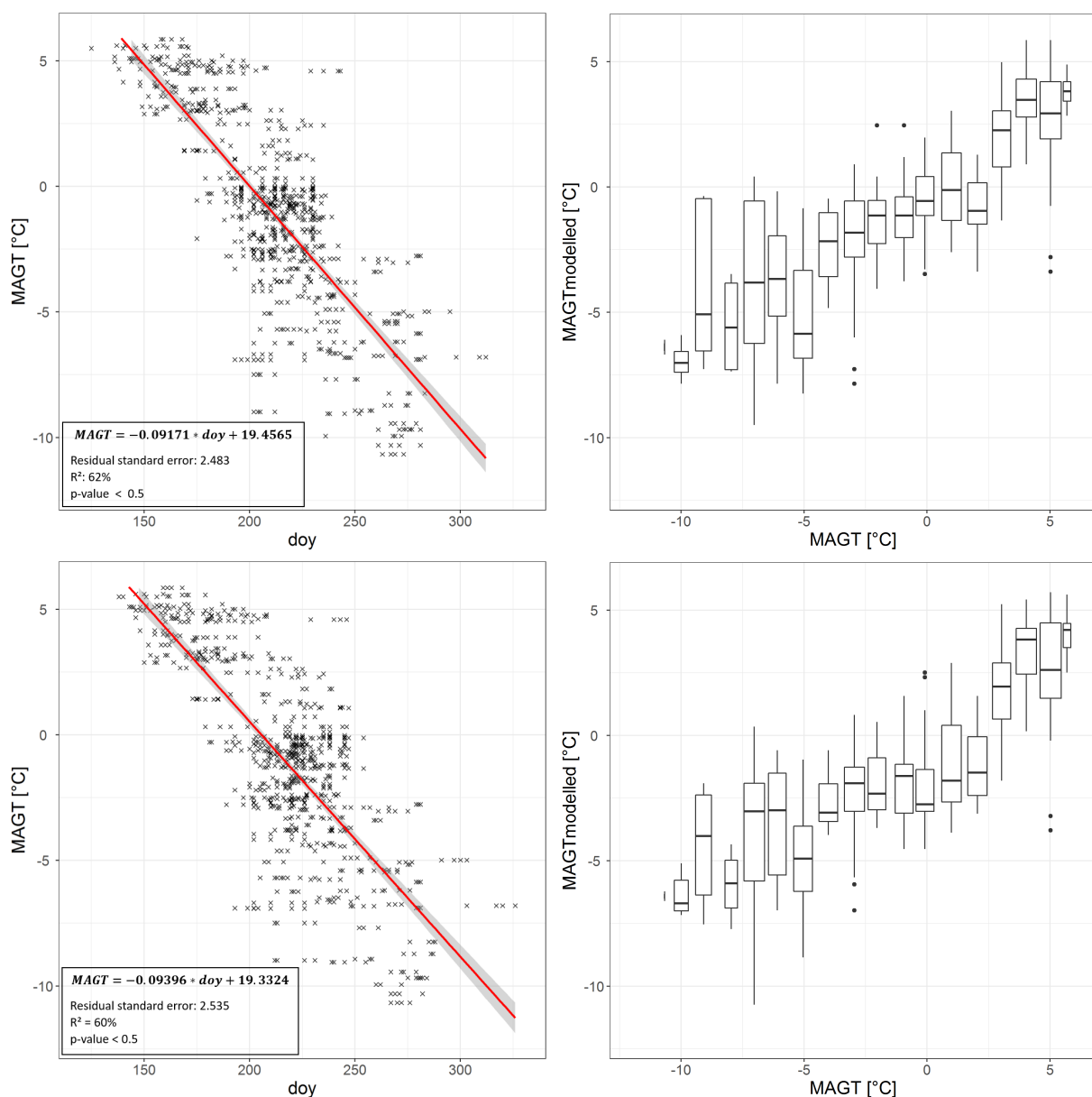
Figure 5. Left: Comparison of number of frozen days (doy - days of year) from Metop ASCAT and Mean Annual Ground Temperature for GTN-P boreholes (at depth of coldest sensor, years 2010-2012). Red line represents linear fit. Right: Box plots of modeled versus Mean Annual Ground Temperature from GTN-P boreholes (at depth of coldest sensor, years 2007/8 and 2008/9) Top: ASCAT excluding snow melt days, bottom: ASCAT with snow melt days.
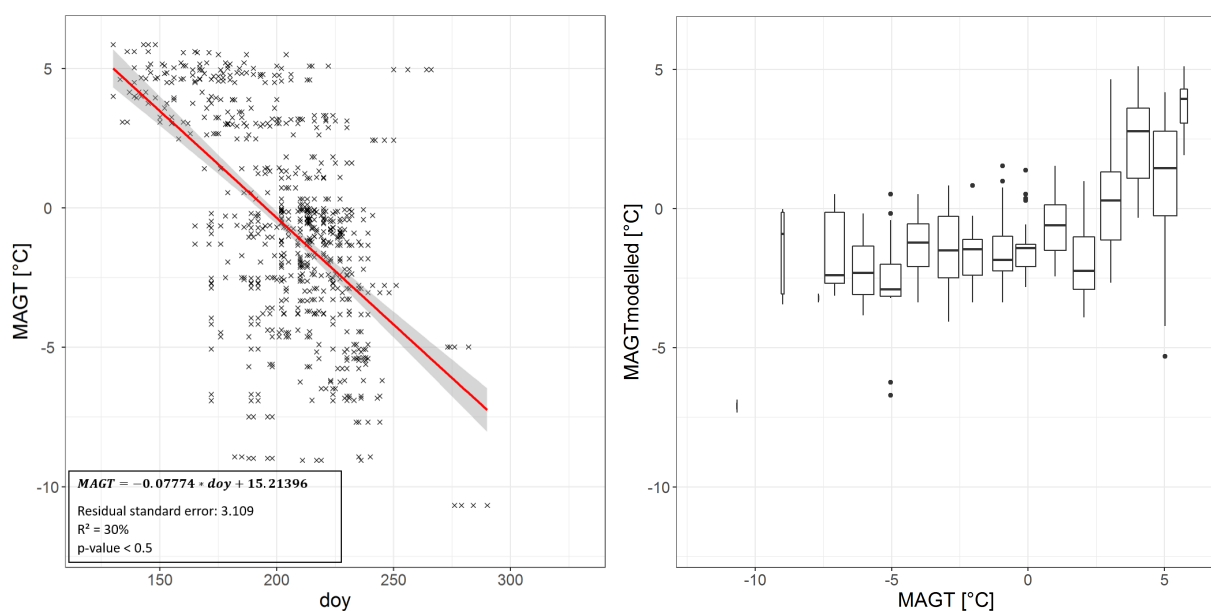
Figure 6. Left: Comparison of number of frozen days (doy - days of year) from SSM/I and Mean Annual Ground Temperature for GTN-P boreholes (at depth of coldest sensor, years 2010-2012). Red line represents linear fit. Right: Box plots of modeled versus Mean Annual Ground Temperature from GTN-P boreholes (at depth of coldest sensor, years 2007/8 and 2008/9).
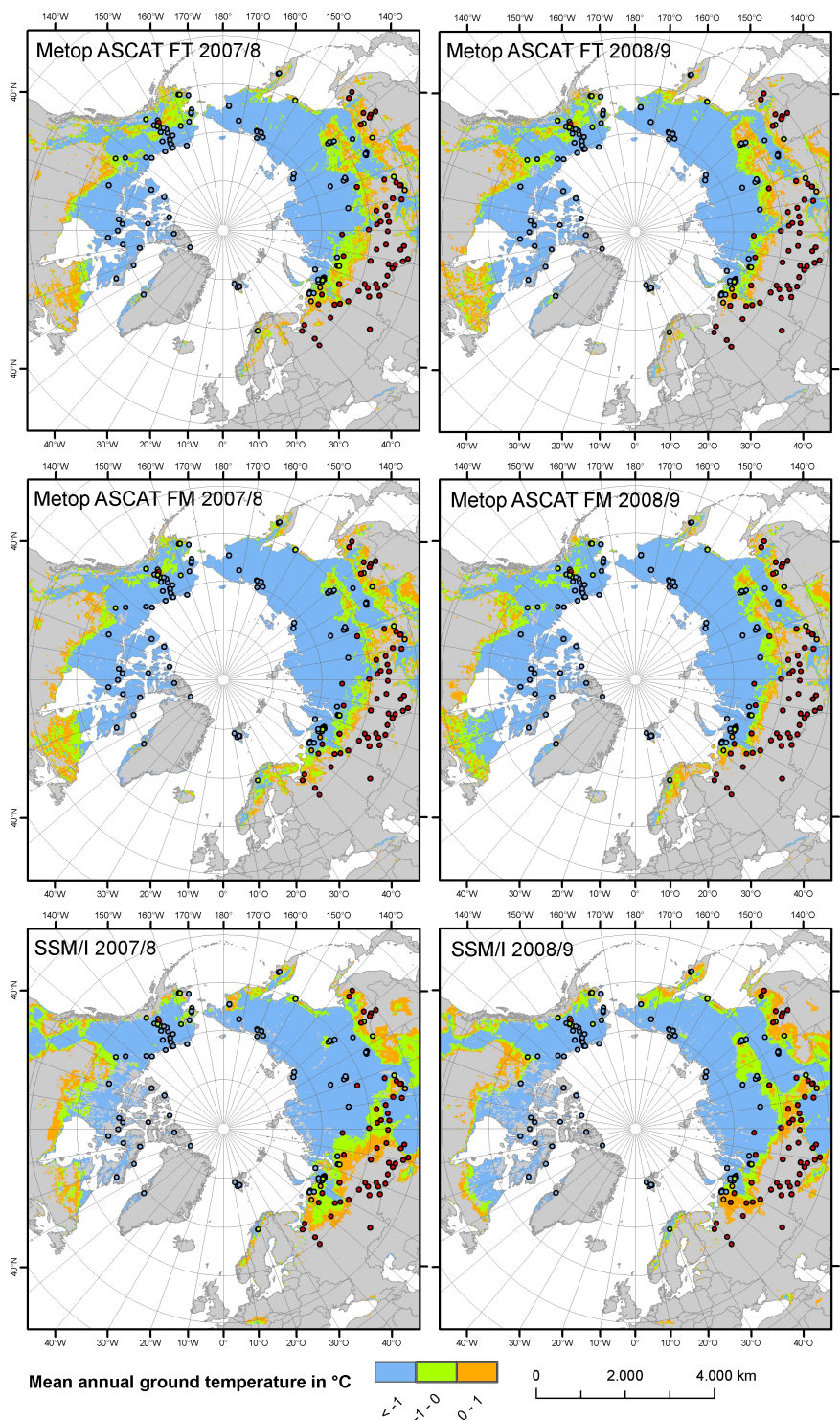
Figure 7. Circumpolar maps of three mean annual ground temperature classes (below -1°, -1° – 0°, 0° – 1°C) from modelling results using ASCAT and SSM/I. FT - days identified as frozen, FM - days with melting snow are considered as frozen ground in ASCAT. Locations of boreholes with in situ data are shown as circles. Color coding corresponds to satellite classes.
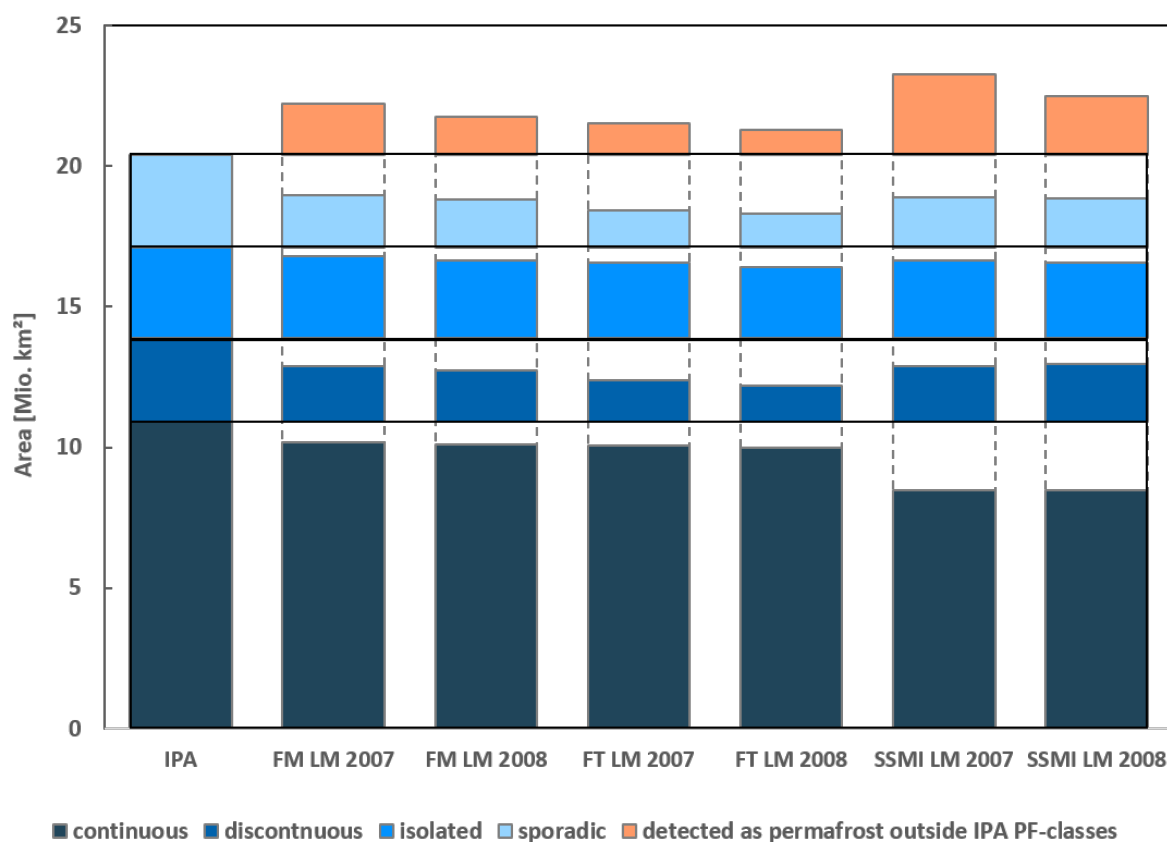
Figure 8. Permafrost extent comparison of satellite data results based on modelled ground temperatures (LM - Linear Model) with permafrost classes from Brown et al. (1997). Covered area in km^2 within each class and outside. FT - days identified as frozen with ASCAT, FM - days with melting snow are considered as frozen ground with ASCAT.
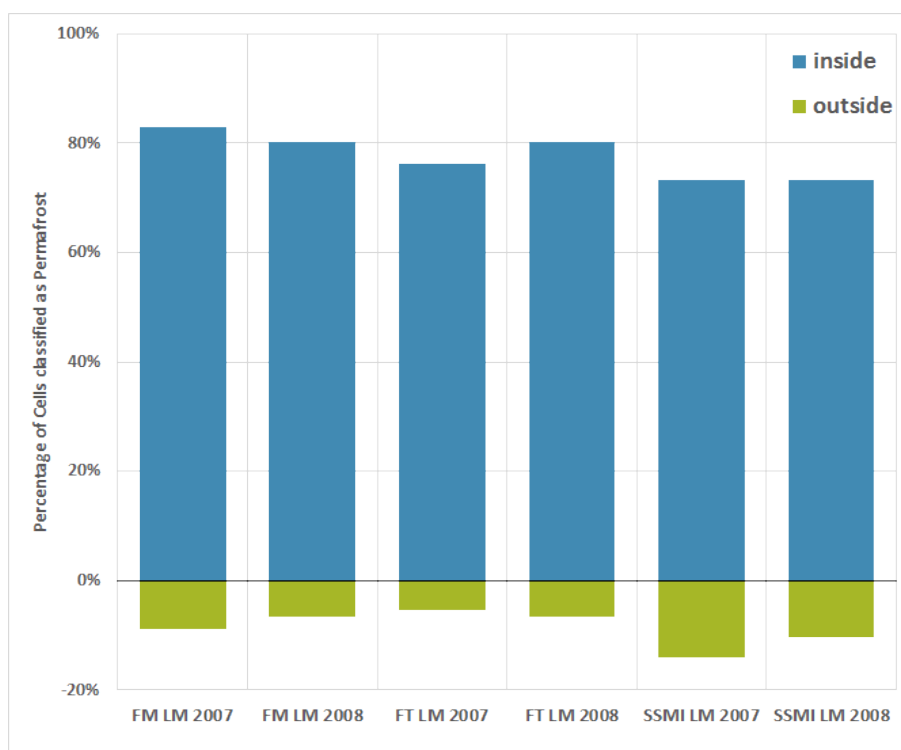
Figure 9. Comparison of satellite data results based on based on modelled ground temperatures with permafrost extent from Brown et al. (1997). Covered area in % inside and outside permafrost regions. FT - days identified as frozen without melting snow are used, FM - days with melting snow are considered as frozen ground, LM - model results.
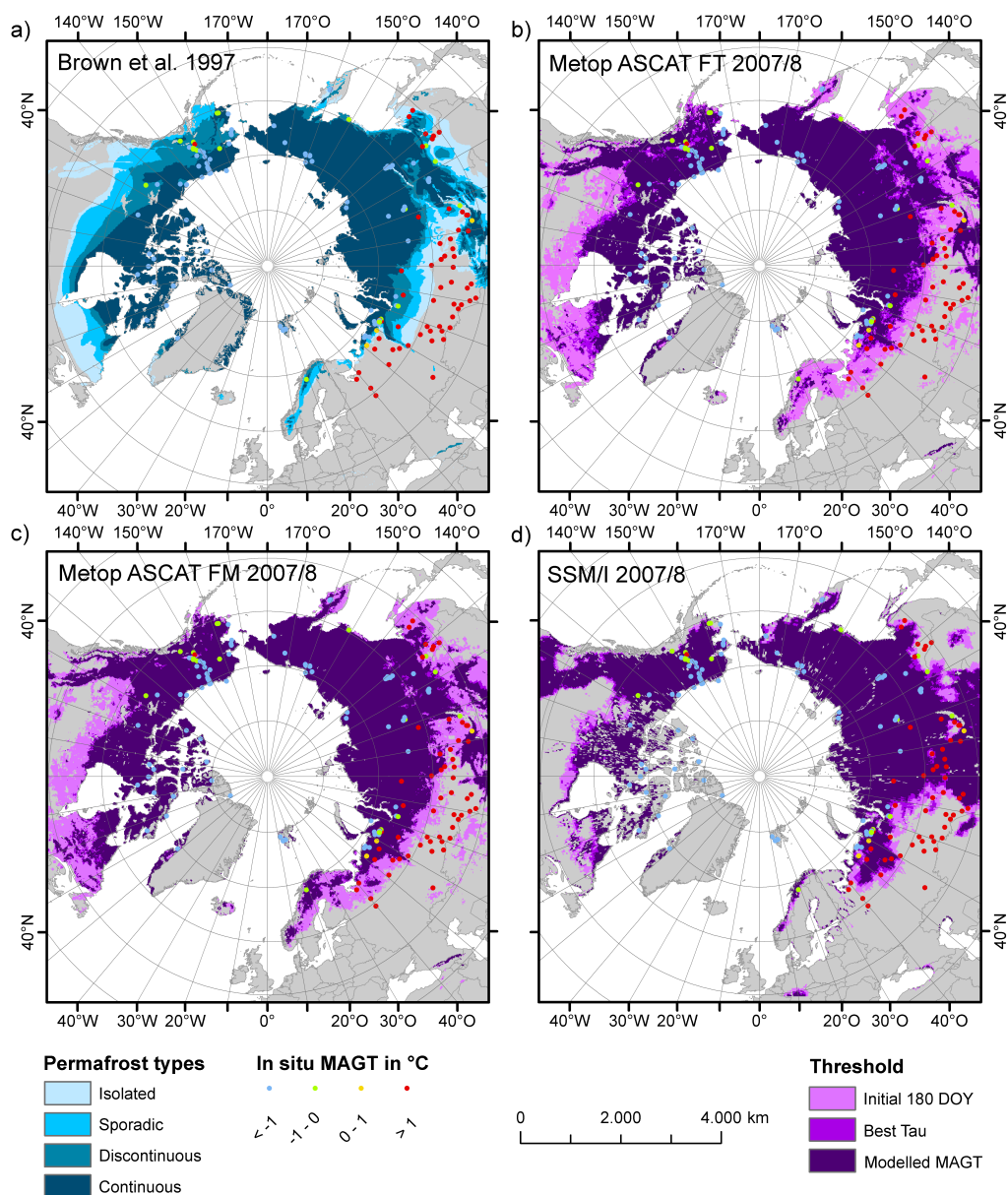
Figure 10. Permafrost extent maps based on a) permafrost extent classes from Brown et al. (1997), b) thresholds applied to frozen days of year (DOY) to ASCAT excluding melt days, c) thresholds applied to frozen days of year (DOY) to ASCAT including melt days, and d) thresholds applied to frozen days of year (DOY) to SSM/I. The initial threshold is 180 days. The value for best Kendall's τ represents the best fit with borehole measurements. The highest threshold has been determined using an empirical model calibrated with borehole measurements. See also Table 2. All satellite results are based on 2007/8-2008/9 records.
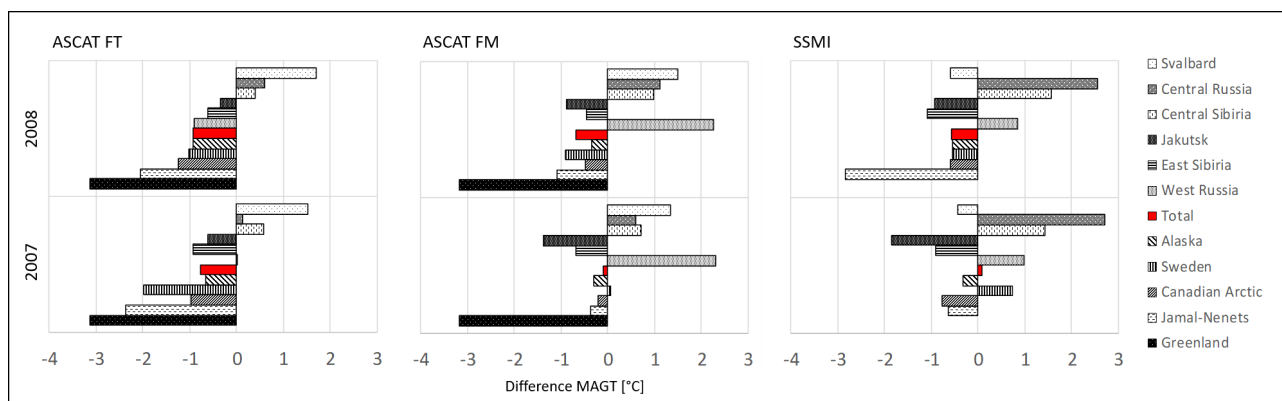
Figure 11. Difference between in situ MAGT (coldest sensor) and modelled MAGT by region (see Fig. A1) in 2007/8 and 2008/9. FT - days identified as frozen without melting snow are used, FM - days with melting snow are considered as frozen ground in ASCAT.

Appendix A
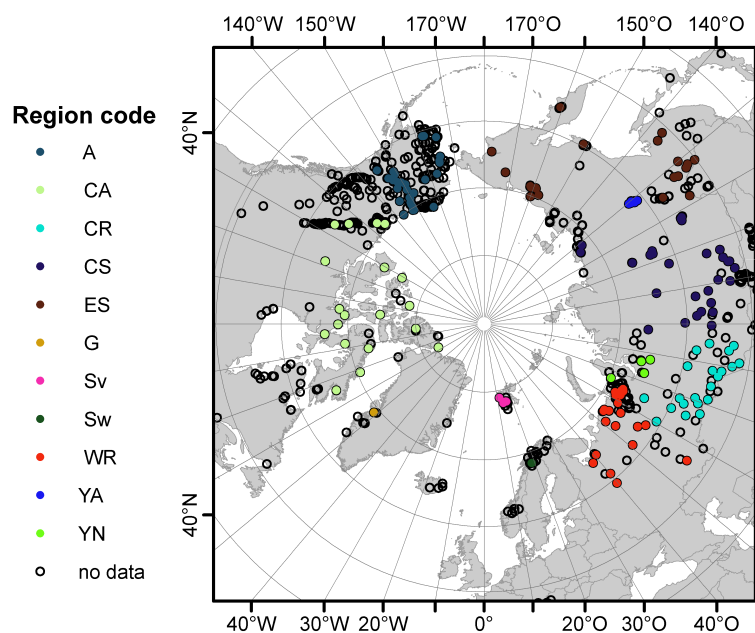
Figure A1. Map of used GTN-P boreholes with region class. 'No data' refers to sites without publicly available data or sites which failed the selection criteria. A - Alaska, CA - Canada, CR - Central Russia, CS - Central Siberia, ES - Eastern Siberia, G - Greenland, Sv - Svalbard, Sw - Sweden, WR - Western Russia, YA - Yakutia, YN - Nenets.
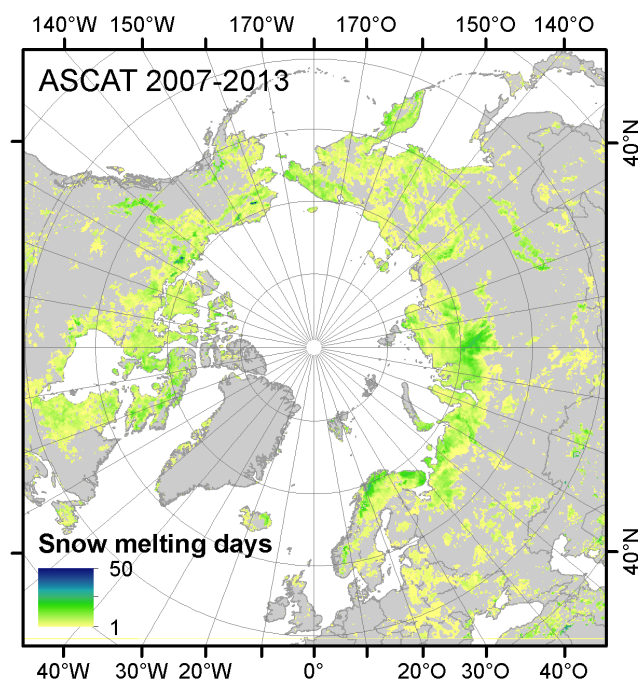
Figure A2. Average number of snow melting days per year from Metop ASCAT for 2007 – 2013 derived from Paulik et al. (2014).